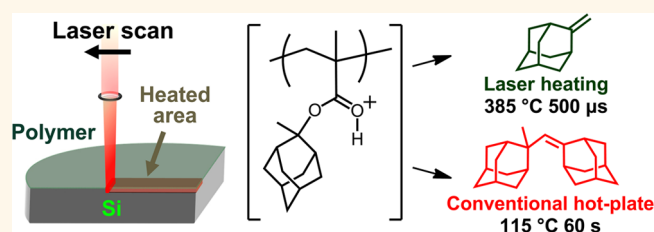


Laser-Induced Sub-millisecond Heating Reveals Distinct Tertiary Ester Cleavage Reaction Pathways in a Photolithographic Resist Polymer

Byungki Jung,[†] Pratima Satish,[†] David N. Bunck,[‡] William R. Dichtel,[‡] Christopher K. Ober,[†] and Michael O. Thompson^{†,*}

[†]Department of Materials Science and Engineering and [‡]Department of Chemistry and Chemical Biology, Cornell University, Ithaca, New York 14853, United States

ABSTRACT Acid-catalyzed, thermally activated ester cleavage reactions are critical for lithographic patterning processes used in the semiconductor industry. The rates of these high-temperature reactions within polymer thin films are difficult to characterize because of the thermal instability of many polymers and a lack of temperature-resolved measurement techniques. Here we introduce the use of transient laser irradiation to heat a methyladamantane-protected acrylate copolymer to 600 °C in less than a millisecond. These conditions mediate the removal of the protecting groups and enable accurate kinetic measurements. At sub-millisecond exposure to high temperatures (~600 °C), the rate of the ester cleavage reaction exhibits the expected first-order dependence on acid concentration. In contrast, the reaction exhibits more complex kinetics when the polymer film is heated to lower temperatures (115 °C) on a conventional hot-plate. We identify distinct methyladamantane-derived deprotection products under the high- and low-temperature conditions that are consistent with the observed rate differences. The acid-catalyzed dimerization of 1-methylenadamantane occurs at low temperature, which reduces the acid concentration available for the ester cleavage. This dimerization reaction is minimized during transient laser-induced heating because bimolecular reactions are disfavored under these conditions. We constructed a mathematical model based on these observations that accounts for the competition for the catalyst between the dimerization and ester cleavage processes. This laser-induced, sub-millisecond heating technique provides a means to probe and model temperature and time regimes of thermally activated reactions in polymer films, and these regimes exhibit distinct and advantageous reaction pathways that will inform future advances in high-performance photolithography.



KEYWORDS: chemical reaction kinetics · deprotection · acid diffusion · resist polymer · laser spike annealing · rapid thermal processing

Over the past four decades, photolithography has enabled advances in sub-micrometer scale patterning technology, leading to faster computing and advances in the microelectronics industry. Lithography involves patterning a radiation-sensitive polymer, known as a photoresist, which protects the underlying substrate during subsequent etching steps. Chemically amplified photoresists have been used for three decades for deep ultraviolet (DUV) lithography because of their high sensitivity and excellent patterning performance. Chemical amplification involves photochemically generating a strong acid in the resist film, which cleaves (deprotects) the esters along the polymer backbone during a subsequent

heating step referred to as the postexposure bake (PEB). The resist's solubility changes upon deprotection, facilitating its selective removal with a developing solvent.^{1,2} Resist materials face numerous challenges as pattern dimensions approach sub-15 nm length scales, including control of the diffusion of the acid catalyst during PEB. To predict and optimize the resist performance, reaction pathways must be fully understood at the molecular level and interaction kinetics between the relevant species must be mathematically modeled. One of the key challenges is that these processes are difficult to study over a broad temperature range because of the resist's limited thermal stability.

* Address correspondence to mot1@cornell.edu.

Received for review January 27, 2014 and accepted May 13, 2014.

Published online May 13, 2014
10.1021/nn500549w

© 2014 American Chemical Society

Conventional PEB involves heating substrates to 90–150 °C for 30–120 s with temperature ramp rates on the order of 100 K/s. In contrast, continuous wave (CW) laser heating sources can transiently heat thin polymer films to more than 400 °C above their conventional decomposition temperatures, providing access to new kinetic regimes with rates spanning 8 orders of magnitude.³ This process, known as laser spike annealing (LSA), was first utilized as a millisecond annealing technique to activate dopants while minimizing diffusion in ultrashallow semiconductor junctions.^{4,5} In LSA (Figure 1), a line-focused CW laser is scanned over the substrate to rapidly heat the surface for microseconds to milliseconds, after which cooling occurs quickly through conduction into the substrate. Laser-induced PEB is characterized by rapid heating at 10^4 – 10^5 K/s to peak temperatures of 200–600 °C, such that the ester cleavage reaction requires only 200–2000 μ s to change the resist's solubility.^{3,6} Improvement in pattern quality, quantified by the line edge definition and UV dose (mJ/cm^2) at resolution, was demonstrated using deep UV and extreme UV lithography followed by laser PEB.^{7,8} Here we employ this laser technique to access and characterize different chemical outcomes and kinetic regimes for photolithography.^{9,10}

P(MAdMA-co-GBLMA), a model resist with an adamantyl protecting group used for both deep UV and extreme UV lithography, was investigated over the broad temperature and time range available using hot-plate and LSA heating. Deprotection in this system occurs in the presence of an acid and heat as the adamantyl ester side group is cleaved from the backbone leaving P(methacrylic acid) and methylene adamantane byproducts (Scheme 1).¹¹ While characterizing this ester cleavage over a temperature range from 115 to 560 °C, we observed an unexpected change in the kinetics; the apparent activation energy for ester cleavage decreased by a factor of 3 from 73 ± 11 kJ/mol at conventional hot-plate temperatures (115 to 170 °C) to 21 ± 1 kJ/mol at LSA temperatures (250–560 °C).³ Although we suggested that this could be attributed to changes in acid mobility associated with segmental dynamics of the polymer in the two regimes, we show in this present work that the behavior is more likely coupled to a fundamental change in the reaction mechanism.

The reaction rates and pathways during hot-plate and LSA heating were determined using Fourier transform infrared (FTIR) spectroscopy, NMR spectroscopy, and gas chromatography/mass spectrometry (GC/MS). Results indicate that, at low temperatures and second time frames, the methylene adamantane byproduct undergoes a secondary reaction to form a dimer. This dimer acts as a dynamic acid trap inducing non-exponential reaction kinetics and provides chemical insight to explain previously inconclusive models and

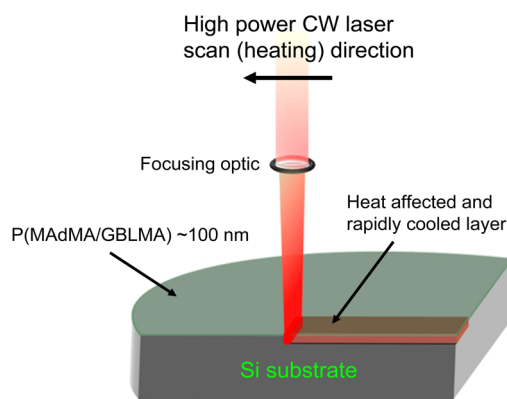


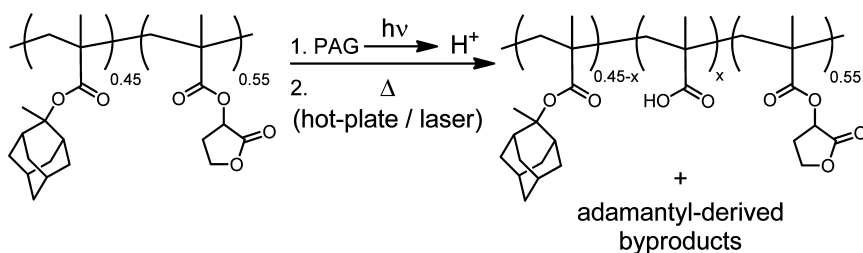
Figure 1. Millisecond characterization method using a line-focused, continuous wave CO_2 laser system. Schematic drawing shows a line-focused CO_2 beam ($100 \mu\text{m} \times 700 \mu\text{m}$) scanning the substrate. The top $100 \mu\text{m}$ of the surface is rapidly heated, subsequently cooling by thermal conduction into the silicon substrate.

simulations. The observation of these different reaction pathways also demonstrates the potential for significant changes in the behaviors of small molecules and polymer systems at extreme temperatures. Ultimately, this chemical insight into the space-resolved reactivity of photoresists will drive continued innovation in nanometer scale patterning that forms the basis of the semiconductor industry.

RESULTS

The rates of MAdMA ester cleavage reactions were measured using either conventional (hot-plate) or laser-induced heating. Acid diffusion and ester cleavage are both thermally activated processes that require only milliseconds at high temperatures (laser), while reactions at lower temperatures require between 30 and 120 s to achieve comparable conversions. The thickness of the polymer film after development was used as a measure of the ester cleavage rate^{12–14} and was determined as a function of heating temperature, time, and the initial acid concentration (UV dose).

In the absence of acid, P(MAdMA-co-GBLMA) resist was stable to much higher temperatures under laser heating conditions as compared to conventional heating. Thermal stability over long time scales (seconds to minutes) was determined by thermogravimetric analysis and by measuring the residual film thickness as a function of temperature and time on a vacuum hot-plate. Figure 2a indicates that both film thickness and polymer mass remain unchanged below 200 °C. A $\sim 60\%$ decrease in polymer thickness and weight percentage is observed above 200 °C, corresponding to the loss of lactone and methyladamantane esters as confirmed by NMR spectroscopy.¹⁵ The methacrylate polymer backbone begins to decompose to form poly(methacrylic acid) above 300 °C (see Supporting Information). In contrast, P(MAdMA-co-GBLMA) is stable to much higher temperature (~ 800 °C) under the short



Scheme 1. Predicted ester cleavage reaction of P(MAdMA-co-GBLMA). The polymer film is heated to initiate an acid-catalyzed reaction, where the adamantyl ester is cleaved and modifies the solubility of the polymer matrix. The adamantyl ester forms a methylene adamantane while generating another acid, which diffuses to cleave additional esters until the heating source is removed.

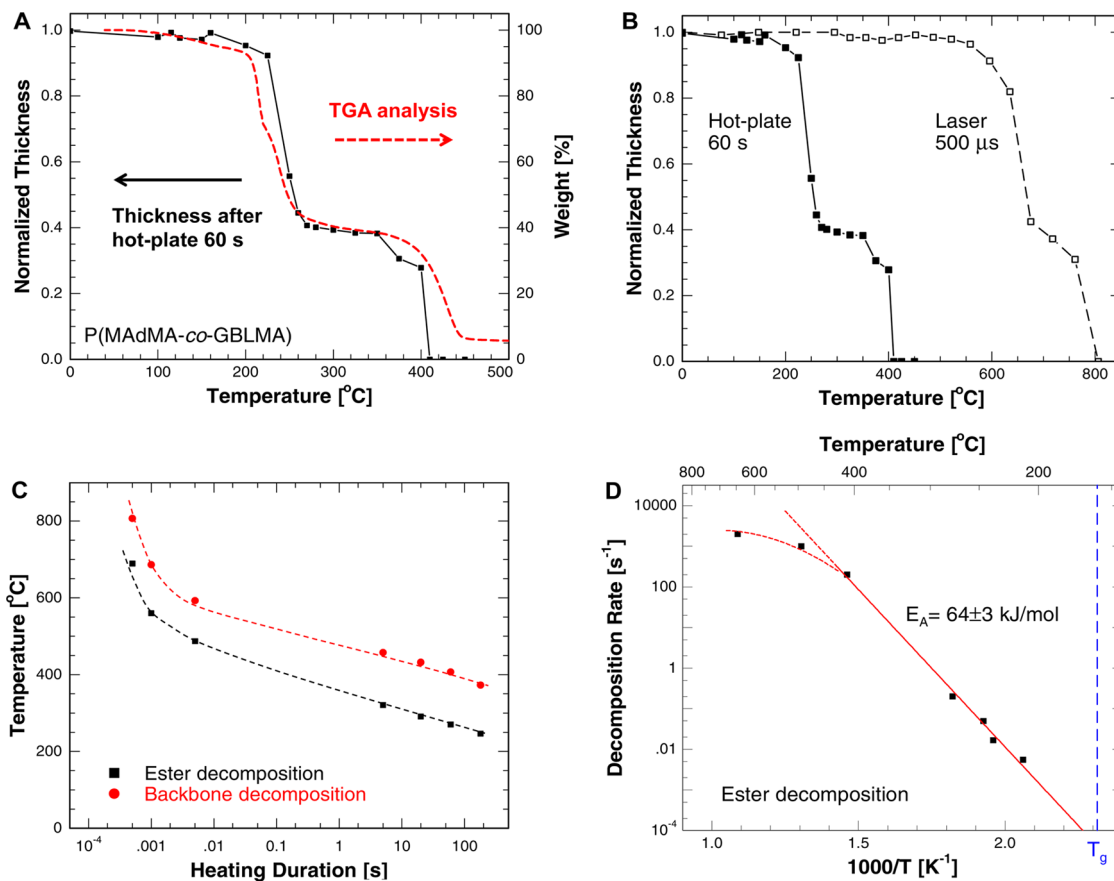


Figure 2. Measured film thickness of intrinsic P(MAdMA-co-GBLMA) to investigate its thermal stability. (A) Film thickness remaining and polymer weight percentage loss as a function of temperature under 60 s hot-plate heating or 5 °C/min TGA. Both film thickness and weight percent yield comparable results. (B) Film thickness showing the thermal stability limits under hot-plate (60 s) and laser-induced (500 μs) heating. Reducing the heating duration by 5 orders of magnitude increases the temperature stability of the polymer by 400 °C. (C) Thermal stability of the C–C backbone and esters as a function of heating duration showing extended thermal stability into millisecond time frames. (D) Decomposition rate ([heating duration]⁻¹ at 30% thickness loss) during the ester loss as a function of inverse temperature.

duration (500 μs) conditions associated with laser heating (Figure 2b), and the stability temperature is inversely proportional to the heating duration (Figure 2c). When the heating duration is shortened to the sub-millisecond regime, the onset temperature for the ester and the backbone decompositions increases significantly. These data demonstrate that organic polymers are stable to much higher temperatures than T_D as measured by TGA when the heating duration is significantly reduced. The rate of polymer decomposition can be estimated as the

inverse of the heating duration at a given thickness loss, as shown in Arrhenius form in Figure 2d.¹⁶ At temperatures above 160 °C ($T_g \approx 159$ °C), decomposition follows Arrhenius behavior with an activation enthalpy $E_A = 61 \pm 2$ kJ/mol, comparable to the cleavage energy of the side group.^{17,18} However, as temperatures exceed ~500 °C, the decomposition rate reaches a maximum value that is insensitive to further temperature increases, as evidenced by the asymptotic temperature stability at sub-millisecond durations shown in Figure 2c.

The critical acid-catalyzed cleavage reaction kinetics were investigated for heating durations ranging from sub-milliseconds to minutes. The rate of ester cleavage was characterized by constructing dissolution curves (Figure 3a), in which the remaining polymer film thickness after development was observed as a function of the initial acid concentration generated by a given UV exposure dose (see Supporting Information). The dose required to remove the entire polymer film (E_0) is a function of both heating time and temperature;¹⁹ representative data are shown for both 60 s hot-plate and 500 μ s laser heating at various temperatures. We constructed isotherms of E_0 versus heating time (Figure 3b) to compare the ester cleavage behavior as a function of temperature and reaction time. At constant temperature, E_0 decreases with increasing heating duration due to the longer time available for the acid-catalyzed ester cleavage. The data suggest a power-law dependence $E_0 \propto t^n$ with different slopes for the two time/temperature regimes: $n = -1$ for milliseconds and $n = -0.25$ for seconds time frame heating.

It has been proposed that the rate of ester cleavage should be governed by the following first-order differential equation:

$$\frac{d\phi}{dt} = k_p H [1 - \phi(t)] \quad (1)$$

in which ϕ is the fraction of cleaved ester, H is the concentration of the UV-generated acid catalysts, and k_p is a reaction rate constant.²⁰ The solution to this equation, $\phi = 1 - e^{-k_p H t}$, reduces to $\approx k_p H t$ for short times. For a given polymer, E_0 corresponds to a specific cleavage fraction $\phi(t)$ where the solubility change is sufficiently large to enable full dissolution during the 60 s development. Similarly, the catalyst concentration H is directly proportional to the UV dose. Consequently, the product of E_0 and the heating duration t should be a constant; that is, increasing the acid concentration (E_0) should reduce the dissolution time proportionately. This interpretation is consistent with $n = -1$ (hence $E_0 \propto t^{-1}$) as was observed under millisecond laser heating.

The power-law slope observed in the millisecond/high-temperature regime was indeed close to unity, consistent with a first-order ester cleavage reaction. As the acid concentration is reduced by a factor of 2, the heating time needed to achieve a comparable change in solubility doubles. However, this relationship is not valid for dissolution experiments performed under long duration/low-temperature conventional heating, in which halving acid concentration increases the required time by a factor of 16. This finding indicates that the deprotection reaction under these conditions,³ comparable to industrial lithography processes, is more complex. Similar behavior was observed with another resist system poly(4-*tert*-butoxycarbonyloxystyrene), whose chemical reactions involve a different mechanism with conversion of a *tert*-butoxycarbonyl group to

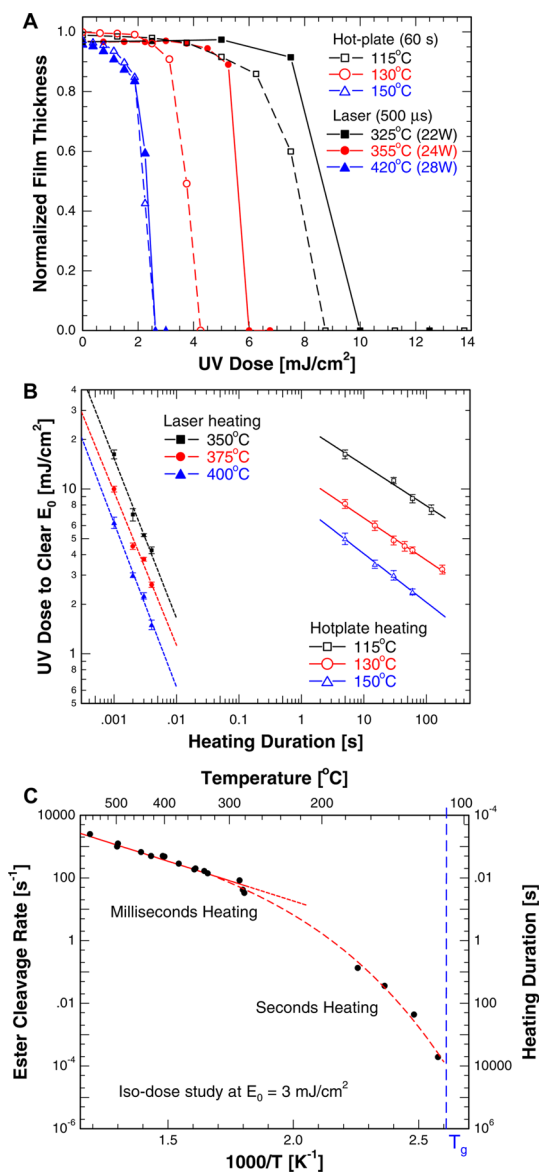


Figure 3. UV exposure dose required to reach the solubility switch and remove the polymer film from the substrate (E_0). The comparison between conventional and laser-induced heating effectively measures the ester cleavage kinetics. (A) Normalized thickness remaining versus dose (proportional to the initial acid catalyst concentration) for hot-plate and 500 μ s laser-induced heating. (B) Isotherms of E_0 versus heating time showing different slopes between two heating conditions, suggesting a change in the ester cleavage reaction kinetics. (C) Ester cleavage rate versus inverse temperature at a fixed E_0 of 3 mJ/cm^2 .

an isobutene (see Supporting Information). Slopes for this resist system were ≈ 0.5 for hot-plate and ≈ 1.1 for laser heating. The simple first-order behavior of the laser regime appears universal, whereas the complex hot-plate kinetic regime may vary with polymer systems and the relative temperature deviation $T - T_g$. For P(MAdMA-co-GBLMA), the transition between these two kinetic regimes (Figure 3c) occurs at approximately 200 °C, which could correspond to slower chain dynamics expected as temperatures approach T_g (~ 110 °C). However,

we have also identified fundamental changes in the ester cleavage reaction that influence this rate,¹⁰ as discussed below.

The net rate of ester cleavage is dependent on both the direct cleavage reaction and the diffusion of the catalytic acids within the matrix. Kang *et al.* proposed a specific acid-catalyzed cleavage mechanism for P(MAdMA-co-GBLMA) (Scheme 1), where methyladamantyl esters are ultimately eliminated to produce methylene adamantane. They also suggested that this reaction should be first-order in $[H^+]$, but they observed nonlinear kinetics which they explained as the result of acid trapping.²¹ Other researchers attempting to model the nonlinearity in the deprotection rate (under hot-plate heating) have proposed a range of chemical mechanisms. These include concentration-dependent acid diffusion, non-exponential distribution of waiting times between acid hopping events,²² acid loss by quenchers and traps,^{21–24} and dynamic free volume changes in the resist.^{21,23,24} Measured acid diffusivities in the P(MAdMA-co-GBLMA) system³ show strong temperature dependence, but there is no evidence of any concentration dependence at either hot-plate or laser-induced temperatures. Similarly, quenchers and extrinsic traps would likely be equally efficacious at both low and high temperatures. These mechanisms cannot explain the kinetic changes between the two regimes.

Acid traps were initially introduced as a phenomenological process where their concentration resulted in nonlinear deprotection levels and rates. Recently, Kang *et al.* proposed P(methacrylic acid) as the specific acid trap in this system, assuming methylene adamantane as the only byproduct.²¹ Fundamental changes in the nature of this acid trap with temperature could well lead to our observed kinetic shift. In addition, any fundamental change in the chemistry of the reaction at high temperatures could also lead to different trapping mechanism and hence different kinetic behavior. Consequently, we sought to characterize the ester cleavage reaction and the resulting molecular byproducts under both heating conditions.

FTIR spectroscopy of the films before and after ester cleavage indicated the expected absorbance corresponding to carbonyl stretches of adamantyl esters, lactones, and/or carboxylic acids (see Supporting Information), which would be consistent for similar reaction pathways. However, FTIR is limited in its ability to identify subtle chemical structure changes and specific cleavage byproducts. In contrast, ¹H NMR analysis of the dissolved, cleaved polymer films indicated substantial differences in the chemical composition of the reaction byproducts as a function of heating method (Figure 4). The spectra of reactions performed under laser irradiation (385 °C, 500 μs) exhibit a sharp singlet at 4.45 ppm that corresponds to methylene adamantane. In contrast, this resonance is greatly

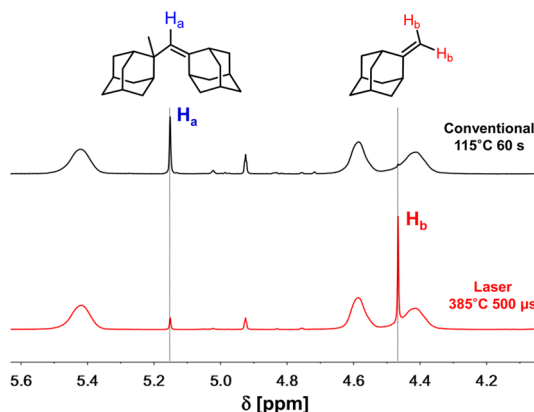


Figure 4. ¹H NMR spectra of P(MAdMA-co-GBLMA) showing chemical shifts after acid-catalyzed ester cleavage reaction using hot-plate at 115 °C for 60 s or laser at 26 W (385 °C) for 500 μs. While locations of the peaks are similar between the two heating methods, significantly different intensities at 4.45 ppm (methylene adamantane) and 5.15 ppm (adamantyl dimer) are observed, suggesting a different concentration and types of adamantyl-derived byproducts formed during the cleavage reactions.

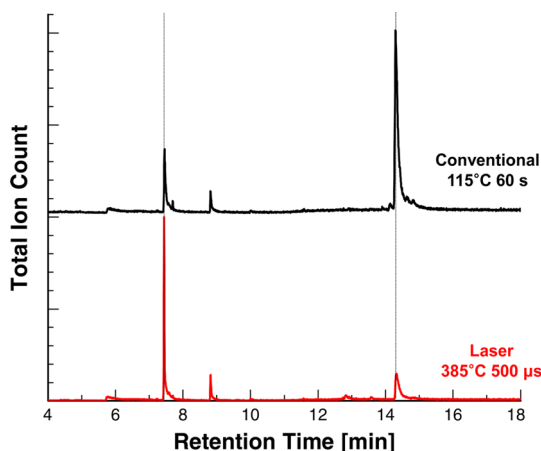


Figure 5. Gas chromatography of P(MAdMA-co-GBLMA) showing the total ion current (TIC) as a function of retention time after acid-catalyzed ester cleavage reaction using laser (top) or hot-plate (bottom). For the two heating methods, significantly different TICs are observed for retention times of 7.5 min (methylene adamantane) and 14.5 min (adamantyl dimer), verifying the ¹H NMR data. The peak at 9.0 min corresponds to 2-methyl-2-adamantanol formed from ambient H₂O.

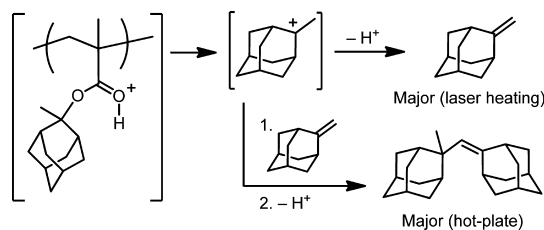
attenuated in spectra of cleavage reactions heated conventionally (115 °C, 60 s). An intense singlet at 5.15 ppm is observed instead, which we have unambiguously assigned as the vinyl proton of a methylene adamantane dimer using ¹H and 2D NMR spectroscopy (Figure S6). These structural assignments and differences in product distributions under the two heating conditions were further confirmed by GC/MS (Figure 5), which reveal significant differences in total ion count (proportional to concentration) for the reaction byproducts at retention times of 7.5 and 14.5 min. The molecular ions and fragmentation patterns of the mass spectra at these retention times correspond to methylene

adamantane and its dimer, respectively (see Supporting Information).

These experiments unambiguously demonstrate that the two heating methods produce very different concentrations of methylene adamantane and adamantyl dimer. Under hot-plate heating, the dominant byproduct is the adamantyl dimer whereas methylene adamantane is primarily observed under laser heating. While deprotection byproducts in other resist systems, such as isobutene in poly(4-*tert*-butoxycarbonyloxy-styrene), can escape the film by evaporation,²⁵ we do not believe this is the case for this system. The boiling point of methylene adamantane is ~ 203 °C, and the estimated vapor pressure at 115 °C is less than 0.1 bar.²⁶ Consequently, outgassing of the byproducts is unlikely. Furthermore, measurements of the total concentration of byproducts after either hot-plate or laser heating are comparable, supporting the conclusion that outgassing of the byproducts is minimal and the differences are intrinsic to the reaction pathways.

The identification of this alternate pathway is surprising given the widespread use of adamantyl esters in commercial photoresists. However, the final reaction byproduct at low temperature has now been identified as primarily the adamantyl dimer with only low concentrations of methylene adamantane. Implications of this change in the reaction pathways on modeling resist performance will be discussed below.

The different reaction outcomes at each heating condition are consistent with the thermodynamic parameters of elimination and dimerization reactions, as well as the limited molecular diffusion lengths that disfavor dimerization under the short duration, local heating laser conditions.²⁷ We also attribute the complexity of the ester cleavage reaction kinetics under conventional heating to competition between the ester cleavage reaction and methylene adamantane dimerization (Scheme 2). The dimerization affects the rate of acid-catalyzed ester cleavage because its cationic intermediates can act as traps for the photogenerated acid (Scheme 3).²⁸ Under laser heating conditions, the ester cleavage reaction occurs with the expected first-order dependence on acid concentration and with methyladamantium cation formation likely as the rate-limiting step. At low temperatures, the dimerization side reaction impacts the apparent reaction order through the acid concentration; the available acid concentration in the polymer film varies as a function of time and ester cleavage rates. Furthermore, the reaction kinetics are also coupled to the slower chain dynamics of the polymer.^{29–31} At temperatures approaching the polymer T_g , chain motion of the polymer is limited and the average relaxation time increases, resulting in an increased and strongly temperature-dependent activation enthalpy for ester cleavage.³⁰ Conversely, chain motion becomes rapid at temperatures exceeding the glass transition by more than 200 °C,



Scheme 2. Proposed reaction and structure of adamantyl dimer formed during seconds time frame heating using a vacuum hot-plate. While the bulky dimers may hinder the acid diffusion, their formation is an undesired reaction to the ester cleavage process, which can act as catalyst trap sites.

which will lower the activation barrier for the acid-catalyzed ester cleavage. This mechanism establishes the temperature-dependent activation enthalpy observed in Figure 3c. We believe that these two mechanisms are the origin of the shift from $n = -1$ at high temperature to $n = -0.25$ at low temperature in the power-law dependence of the heating time required for the solubility switch at a given initial acid concentration (Figure 3b).

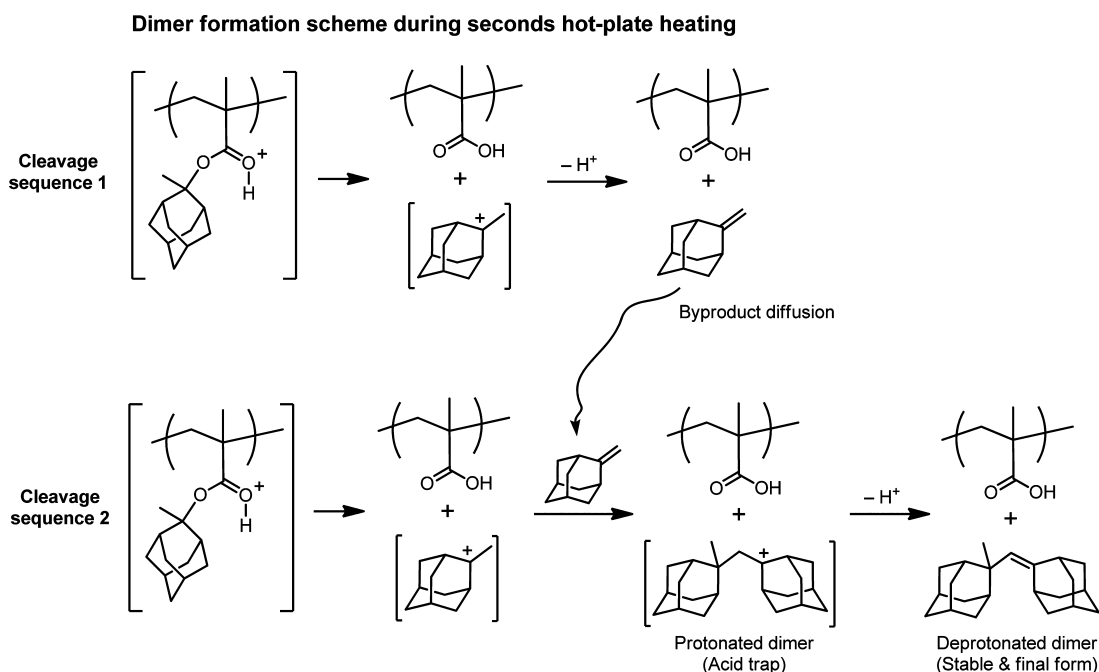
MODELING AND DISCUSSION

Modeling the reaction kinetics with the addition of the dimer formation mechanism and acid trapping on dimer intermediaries introduces substantially increased complexity to eq 1. The ester cleavage rate must now reflect the free acid concentration, which will vary as the concentration of methyladamantane and the dimer changes during the deprotection reaction.

The cleavage of the methyladamantyl ester ultimately forms both methylene adamantane (MA) and dimer byproducts. Previously, the rate of this cleavage reaction was proposed to follow a form given in eq 1. The time/dose dependence at low temperatures strongly suggests that the dimer acts as an acid trap once formed. Consequently, the effective active acid concentration becomes time-dependent and can no longer be modeled as a constant. We denote the free acid concentration as $H(t)$, which is equal to H_0 at $t = 0$. As shown in Scheme 3, the dimer is formed in the protonated state (trapping an acid) and can subsequently transition to a deprotonated form.

To characterize the trapping rates, let C_{MA} be the local concentration of the methylene adamantane, C_{dimer}^* the concentration of protonated adamantyl dimers, and C_{dimer}^0 the concentration of deprotonated adamantyl dimers. In the most general case, and to the degree the activity is proportional to concentration, the rates of dimer formation and methylene adamantane loss are coupled. The fundamental ester cleavage rate equation must be modified to include the time-dependent acid concentration

$$\frac{d\phi}{dt} = k_p H(t) [1 - \phi(t)] \quad (2)$$

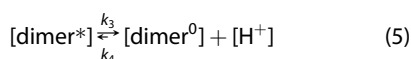
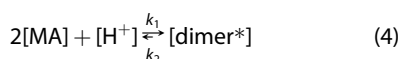


Scheme 3. Detailed reaction pathway for dimer formation during hot-plate heating in seconds time frames. Without the presence of methylene adamantane byproducts, the ester cleavage is a first-order process where methyladamantyl cation immediately releases an acid to form a methylene adamantane byproduct. This byproduct can diffuse in the polymer matrix and react with a nearby methyladamantyl cation, forming adamantyl dimer and delaying the release of the acid catalyst.

where $H(t)$ is the difference between the initial acid concentration and the concentration of protonated dimers.

$$H(t) = H_0 - C_{\text{dimer}}^* \quad (3)$$

The key reactions occurring dynamically include the formation of the protonated dimer and the subsequent deprotonation of the protonated dimer



where it is assumed that only the protonated dimer can decompose back to the methylene adamantane pair. Defining rate constants k_1 and k_2 for the formation and separation of the protonated dimer and rate constants k_3 and k_4 for the dimer protonation and deprotonation reactions, we have

$$\frac{dC_{\text{dimer}}^*}{dt} = k_1 H(t) [C_{\text{MA}}]^2 - k_2 C_{\text{dimer}}^* - k_3 C_{\text{dimer}}^* + k_4 H(t) C_{\text{dimer}}^0 \quad (6)$$

$$\frac{dC_{\text{dimer}}^0}{dt} = k_3 C_{\text{dimer}}^* - k_4 H(t) C_{\text{dimer}}^0 \quad (7)$$

$$\frac{dC_{\text{MA}}}{dt} = C_{\text{MAdMA}} \frac{d\varphi}{dt} - 2k_1 H(t) [C_{\text{MA}}]^2 + 2k_2 C_{\text{dimer}}^* \quad (8)$$

$$= k_p H(t) C_{\text{MAdMA}} [1 - \varphi(t)] - 2k_1 H(t) [C_{\text{MA}}]^2 + 2k_2 C_{\text{dimer}}^* \quad (9)$$

where C_{MAdMA} is the initial concentration of MAdMA esters available for cleavage.

These equations depend critically on the five parameters k_1 , k_2 , k_3 , k_4 , and k_p . Of these constants, only k_p (ester cleavage rate) has been measured directly with a value ranging between 0.5 and 15 nm^3/s over a 20 °C temperature range.²¹ All of these reaction rate constants are expected to follow Arrhenius behavior over the larger temperature range studied here. Several simplifying approximations may be applied to assess the plausibility of this model. We propose that the deprotonated dimer is the thermodynamically stable final state. Consequently, we neglect the reverse reactions with reaction rate constants k_2 and k_4 minimized ($k_2 \rightarrow 0$ and $k_4 \rightarrow 0$). This hypothesis implies that the absence of dimers under high-temperature processing is a kinetic rather than thermodynamic limitation.

The acid trapping efficiency is directly tied to the formation of the protonated dimer and reaction constant k_1 . The secondary reaction (k_3) regenerates the active acid catalyst and allows further deprotection as the acid is released. The ratio k_1/k_p is a critical parameter for establishing the impact of this trap mechanism. For small values of k_1/k_p , the ester cleavage occurs faster than the protonated dimer formation, and the acid concentration does not change significantly. These conditions are fulfilled during high-temperature, short duration laser heating. Since no trapping occurs, the system follows the expected linear first-order kinetics. At lower temperatures and longer heating durations, the k_1/k_p ratio is larger and dimerization occurs at a similar rate as ester cleavage. This effect results in a dynamic depletion of the active acid concentration and

breakdown of linear kinetic behavior, leading to the apparent power-law behavior observed. Ultimately, it is the coupling of the dimer formation with the ester cleavage reaction that leads to the complex kinetic behavior.

The time required to achieve the solubility switch *versus* the acid concentration (UV exposure dose) under isothermal conditions was empirically observed to follow a power-law dependence $E_0 \propto t^n$ (Figure 3b), with $n = -1$ in the laser temperature regime and $n = -0.25$ in the hot-plate temperature regime. The coupled differential equations (eqs 6–9) were numerically integrated to determine the time required to achieve an ester cleavage level of $\phi = 70\%$, the approximate deprotection level required for the solubility switch.¹¹ Results are shown in Figure 6, where the required acid to ester ratio is shown as a function of the time required to reach the solubility switch for a range of k_1/k_p values and k_3/k_p values.

The time scale for the ester cleavage is determined primarily by k_p , where the time shifts inversely with changes in k_p . For this graph, a value of $k_p = 6.5 \text{ nm}^3/\text{s}$ was estimated from experimental measurements at a bake temperature of $110 \text{ }^\circ\text{C}$.²³ Reverse reaction rate constants, k_2 and k_4 , were set to zero corresponding to thermodynamically stable products from the forward reactions. To avoid complete trapping of acids in the dimer, k_3/k_p was set to 0.001, 0.01, or 0.1.

The key parameter is the ratio of the rate of dimer formation to that of ester cleavage k_1/k_p , which will be a strong function of temperature. As $k_1/k_p \rightarrow 0$, the system approaches simple first-order linear kinetics with the dose and time inversely related to each other. We believe that this corresponds to the conditions under laser heating in the sub-millisecond time frame.

As the ratio k_1/k_p approaches unity (low-temperature regime), the rates of dimer formation and ester cleavage are comparable. Under these conditions, the active acid concentration becomes time-dependent and the average is reduced. At high acid concentrations, the cleavage reaction is effectively complete before dimers begin to form, resulting in the asymptotic approach to the $k_1/k_p = 0$ curve. At very low acid concentrations, dimer formation is favored and the effective acid concentration is determined by the transition to the deprotonated dimer, resulting in a much slower net ester cleavage rate. As k_1/k_p is increased further, the critical acid concentration for transition between these two regimes increases.

At both high and low acid concentrations, the curves approach an inverse relationship between the time and the acid concentration (below 1 s and above 100 s). However, the relationship in the transition exhibits much shallower slopes (exponent n). At an acid to ester ratio of 0.1, the slope of the nonlinear region in Figure 6b is approximately $n = -0.3$, which is comparable to the $n = -0.25$ slope experimentally observed (Figure 3b).

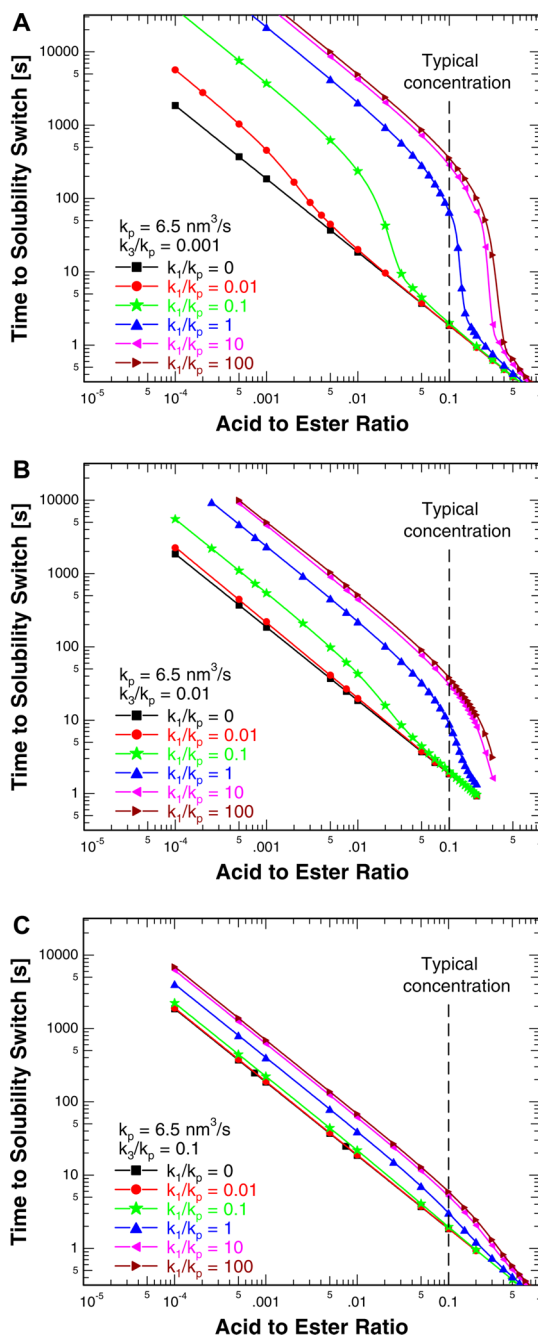


Figure 6. Simulated ester cleavage kinetics using the new mathematical model. The coupled differential equations were numerically integrated to determine the time required to achieve the solubility switch as a function of acid concentration for a range of k_1/k_p and k_3/k_p values: (a) $k_3/k_p = 0.001$, (b) $k_3/k_p = 0.01$, and (c) $k_3/k_p = 0.1$. In each, the transition corresponds to shifting the rate-limiting mechanism for ester cleavage. Once in the trapping regime, the rate returns to proportional to the effective acid concentration set by k_3/k_p .

The transition corresponds to a shift in the rate-limiting mechanism for ester cleavage. At low k_1/k_p values, the cleavage reaction is simply limited by the diffusion of active acids. However, at high k_1/k_p values, release of acids from the protonated dimer effectively determines the cleavage rate. As k_1 and k_p will exhibit

different activation energies, transition from the low to high k_1/k_p regime with temperature is reasonable. Indeed, the modeled rate equations and their simulation are a powerful tool to predict the ester cleavage kinetics.

The parameter k_3/k_p establishes the rate at which protonated dimers release the acid, enabling the catalytic reaction to proceed further. At low values of k_3/k_p , the protonated dimers are increasingly stable and the deprotection level falls rapidly as available acid catalysts are removed from the system. As k_3/k_p increases, the protonated dimer rapidly releases the trapped acid and ultimately becomes equivalent to a system with no dimer trapping mechanism. This behavior is illustrated in Figure 6a,c, showing the same simulations but for k_3/k_p ratios of 0.001 (an order of magnitude slower) and 0.1 (an order of magnitude faster), respectively. To first-order, there is a strong correlation between the kinetic transition and a different set of k_3/k_p values, but the strong power-law dependence for deprotection does not change. While the absolute rate constants are not known, these results confirm that this mechanism can readily explain the observed shift in exponent between laser and hot-plate regimes.

CONCLUSIONS

Cleavage kinetics, decomposition behavior, and reaction pathways of a model photoresist polymer containing a methyladamantyl ester acid-labile group have been extensively studied over a >500 °C window using transient laser-induced heating. The measured ester cleavage rates show non-Arrhenius behavior over the 8 orders of magnitude in kinetic rates studied. While the ester cleavage kinetics were measured to be first-order at high-temperature millisecond heating, they were more complex and exhibited a power-law behavior when the films were heated near T_g for a few seconds. Different molecular byproducts were formed under each condition. At high temperatures, ester cleavage predominantly forms methylene adamantane. In contrast, longer duration conventional heating

at lower temperatures produces an adamantyl dimer, which is identified for the first time. This compound is a likely contaminant that limits the lithographic performance of these resist systems.

The change in kinetics is proposed to originate from the formation of a protonated dimer acting as a catalyst trap, which decreases the active acid concentration available for ester cleavage. This hypothesis is consistent with a new mathematical model that includes both methylene adamantane and adamantyl dimer formations and that reproduces the experimentally observed ester cleavage kinetics. At laser-induced high temperatures, the suppressed dimer formation results in a fixed concentration of active acid catalyst, giving rise to first-order cleavage kinetics. Under conventional heating conditions, the active acid concentration is effectively decreased as a consequence of protonated adamantyl dimer formation, complicating the kinetics of the ester cleavage reaction. Laser-induced heating can be utilized to investigate otherwise unattainable temperatures and kinetic regimes within polymer films and also provides a means to bypass undesirable processes occurring under conventional heating methods.

This work highlights the utility of the laser-induced sub-millisecond heating technique to characterize reaction rates and pathways over a wide range of temperature and time. For lithography, this capability provides critical understanding of catalyst utilization and trapping mechanisms that limit patterning performance, which will contribute to next-generation photoresist design. In addition, laser-induced heating permits direct measurements of previously estimated kinetics and can validate predicted models at extreme temperatures.^{9,10} When combined with existing methods to identify the chemical structure of these polymers, the laser-induced heating technique opens up new opportunities to study chemical processes at high temperatures, and we anticipate that this capability will prove useful for a diverse range of applications beyond photoresist polymers.

MATERIALS AND METHODS

Millisecond Heating. Resist films were irradiated using a CO₂ laser ($\lambda = 10.6$ μm) focused to a ~ 100 $\mu\text{m} \times \sim 700$ μm line beam scanned at velocities of 13–2000 mm/s. These conditions correspond to dwell times (τ_{dwell}) of 7500 to 50 μs , where τ_{dwell} is defined as the beam full width half-maximum divided by the scan velocity. For thin-film polymers, the substrate temperature profile is never entirely isothermal but remains within 5% of the peak temperature for approximately τ_{dwell} and cools to the ambient within $\sim 10\tau_{\text{dwell}}$.⁶ Although polymers are generally poor thermal conductors ($D_T \sim 10^{-4}$ – 10^{-3} cm^2/s), the characteristic thermal diffusion distance for a 500 μs dwell is 200 μm , resulting in nearly complete isothermal equilibration across a 100 nm thick polymer film.

Sample Preparation and Acid Generation Using UV Exposure. The model resist system, 2-methyl-2-adamantyl methacrylate-co- γ -butyrolactone-2-yl methacrylate (MAdMA-co-GBLMA),

was studied over a temperature range from 115 to 560 °C and times from 200 μs to 180 s. The extreme sensitivity of this system to temperature and time made it an ideal candidate for kinetic investigations. P(MAdMA-co-GBLMA) is a chemically amplified photoresist in which acid-catalyzed cleavage of the methyladamantyl protecting group from the methacrylate backbone changes the solubility of the polymer matrix leading to pattern formation. The rate of the cleavage reaction depends on the concentration of acid catalysts within the film, which are generated by ultraviolet (UV) exposure of a molecular photoacid generator (PAG).^{1,2} The UV exposure establishes an initial acid concentration which must be followed by heating to temperatures above 90 °C to thermally activate the ester cleavage reaction as shown in Scheme 1. Stabilization of the byproduct leads to a regeneration of the acid; this regenerated acid diffuses in the polymer matrix to another methyladamantyl

protecting group resulting in a chemical amplification of the cleavage reaction. This heating is conventionally performed on a hot-plate at 90–150 °C for 30–120 s. Using a CW laser heating source, the temperature and time range were extended to temperatures of 560 °C with times correspondingly reduced to 200 μ s.

P(MADMA-co-GBLMA) and triarylsulfonium hexafluoroantimonate salt³² (THSb) were obtained from Mitsubishi Rayon Co., Ltd. and Sigma-Aldrich. P(MADMA-co-GBLMA) was used as a model polymer because of its relatively high glass transition temperature ($T_g \approx 159$ °C)¹² though THSb plasticizes P(MADMA-co-GBLMA) such that the effective T_g of the mixture was ~ 110 °C (see Supporting Information). The as-tested resist system contained P(MADMA-co-GBLMA) blended with 5 wt % THSb in propylene glycol monomethyl ether acetate (PGMEA) solvent for spin-casting.

Polymer films 100 nm in thickness were spun onto Si wafer substrates. These films were subjected to a soft bake process on a vacuum hot-plate at 130 °C for 90 s to remove residual PGMEA solvent. The resist was subsequently exposed to deep UV irradiation ($\lambda = 235$ –260 nm) at doses of 0.1–12 mJ/cm² to generate acid catalysts from the THSb PAG. Following either hot-plate or laser heating to induce cleavage of the MADMA esters, samples were developed using tetramethylammonium hydroxide (TMAH, 0.26 N) for 60 s at 23 °C to remove polymer in the irradiated areas. The fraction of the film removed during the 60 s development is a direct measure of the degree of the ester cleavage reaction.^{12–15}

Polymer Characterization. NMR spectroscopy was performed on a Varian Inova 600 MHz NMR spectrometer using a ¹H{¹³C, ¹⁵N} Z-PFG probe with a 20 Hz sample spin rate. The molecular deprotection products were analyzed using heteronuclear single-quantum correlation and total correlation spectroscopy (HSQC-TOCSY) experiments to decouple ¹³C and ¹H resonances. GC/MS was performed on a JEOL GCmate GC/MS double-focusing mass spectrometer. Fourier transform infrared spectroscopic measurements were performed on a Bruker Hyperion 2000 with Tensor 27 in both transmission and reflection mode. Thermogravimetric and differential thermal analysis was performed using an Exstar TG/DTA 6200 by Seiko Instruments Inc.

Laser Temperature Calibration. The resistance change of a thin-film (50 nm) platinum resistor (thermistor) was used to calibrate the substrate temperature as a function of incident laser power. The thermistors were fabricated on equivalent Si wafers with an area ($<10^{-5}$ cm²) that minimally perturbed the incident laser.⁶ The resistance of Pt is directly proportional to the substrate temperature and was measured with >10 kHz bandwidth. Absolute temperatures were calibrated to experimentally observed melting of silicon (1414 °C) and of micrometer-size Au thin-film dots (1064 °C; see Supporting Information).

Heat Treatment. Photogenerated acids were introduced by exposing resist-coated wafers to UV irradiation. To complete the ester cleavage reaction, samples were subsequently heated under either isothermal conditions on a vacuum hot-plate or using the millisecond laser heating system. In the presence of free acids and sufficient temperature/time, MADMA ester is cleaved and converted to a methyladamantium, which subsequently regenerates the acid as it stabilizes to methylene adamantane (Scheme 1). Three critical properties for this polymer system were measured: the thermal stability of the polymer at extreme temperatures, the solubility switch kinetics *via* dissolution measurements, and the ester cleavage reaction mechanism through spectroscopic measurements.

Conflict of Interest: The authors declare the following competing financial interest(s): Michael O. Thompson is a consultant for Ultratech, a company involved in manufacturing equipment for millisecond annealing. The outcome of this research may be of interest to, or may be beneficial to, Ultratech. The authors declare no other competing financial interest." to replace what currently exists.

Acknowledgment. We gratefully acknowledge Mitsubishi Rayon America Inc. (Taro Ishii), Cornell NMR Facility (Ivan Keresztes), and Intel Corporation (Manish Chandhok and Todd Younkin) for helpful discussions and critical assistance.

We also thank Jing Jiang, Gengqiang Qi, Brandon Wenning, and David Calabrese for experimental support. D.N.B. acknowledges the NSF for a Graduate Research Fellowship. This work made use of facilities in the Cornell NMR Facility (NSF-CHE 7904825; NSF-PGM 8018643), Cornell Center for Materials Research (NSF-DMR 0520404), and the Cornell Nanoscale Facility (NSF-ECS 0335765). Work at Cornell was supported by Intel Corporation and Semiconductor Research Corporation (Task ID: 2125.001).

Supporting Information Available: Decomposition behavior of intrinsic P(MADMA-co-GBLMA) measured using NMR spectroscopy, glass transition temperature measurements, temperature measurement of laser heating, chemical reaction kinetics of P(*tert*-butyl acrylate 4-hydroxystyrene) using laser or hot-plate heating, detailed FTIR, NMR, and mass spectrometry analysis included. This material is available free of charge *via* the Internet at <http://pubs.acs.org>.

REFERENCES AND NOTES

- Ito, H. Chemical Amplification Resists for Microlithography. *Adv. Polym. Sci.* **2005**, *172*, 27–245.
- Ito, H.; Willson, C. G. Chemical Amplification in the Design of Dry Developing Resist Materials. *Polym. Eng. Sci.* **1983**, *23*, 1012–1018.
- Jung, B.; Sha, J.; Paredes, F.; Chandhok, M.; Younkin, T. R.; Wiesner, U.; Ober, C. K.; Thompson, M. O. Kinetic Rates of Thermal Transformations and Diffusion in Polymer Systems Measured during Sub-millisecond Laser-Induced Heating. *ACS Nano* **2012**, *6*, 5830–5836.
- Talwar, S.; Markle, D.; Thompson, M. Junction Scaling Using Lasers for Thermal Annealing. *Solid State Technol.* **2003**, *46*, 83–86.
- Yamamoto, T.; Kubo, T.; Sukegawa, T.; Takii, E.; Shimamune, Y.; Tamura, N.; Sakoda, T.; Nakamura, M.; Ohta, H.; Miyashita, T.; *et al.* Junction Profile Engineering with a Novel Multiple Laser Spike Annealing Scheme for 45-nm Node High Performance and Low Leakage CMOS Technology. *IEEE Int. Electron Devices Meet.* **2007**, *1*, 143–146.
- Iyengar, K.; Jung, B.; Willemann, M.; Clancy, P.; Thompson, M. O. Experimental Determination of Thermal Profiles during Laser Spike Annealing with Quantitative Comparison to 3-Dimensional Simulations. *Appl. Phys. Lett.* **2012**, *100*, 211915-1-3.
- Jung, B.; Ober, C. K.; Thompson, M. O.; Younkin, T. R.; Chandhok, M. Addressing Challenges in Lithography Using Sub-millisecond Post Exposure Bake of Chemically Amplified Resists. *Proc. SPIE* **2011**, *7972*, 797219.
- Krysak, M.; Jung, B.; Thompson, M.; Ober, C. K. Investigation of Acid Diffusion during Laser Spike Annealing with Systematically Designed Photoacid Generators. *Proc. SPIE* **2012**, *8325*, 83250M.
- Debenedetti, P. G.; Stillinger, F. H. Supercooled Liquids and the Glass Transition. *Nature* **2001**, *410*, 259–267.
- Chen, K.; Saltzman, E. J.; Schweizer, K. S. Segmental Dynamics in Polymers: From Cold Melts to Ageing and Stressed Glasses. *J. Phys.: Condens. Matter* **2009**, *21*, 503101.
- Rao, A.; Kang, S.; Vogt, B. D.; Prabhu, V. M.; Lin, E. K.; Wu, W. L.; Turnquest, K.; Hinsberg, W. D. The Deprotection Reaction Front Profile in Model 193nm Methacrylate-Based Chemically Amplified Photoresists. *Proc. SPIE* **2006**, *6153*, 615310.
- Kang, S.; Vogt, B. D.; Wu, W. L.; Prabhu, V. M.; VanderHart, D. L.; Rao, A.; Lin, E. K. Characterization of Compositional Heterogeneity in Chemically Amplified Photoresist Polymer Thin Films with Infrared Spectroscopy. *Macromolecules* **2007**, *40*, 1497–1503.
- Okoroanyanwu, U. *Chemistry and Lithography*; John Wiley & Sons: Hoboken, NJ, 2010; pp 563–603.
- Wallraff, G.; Hutchinson, J.; Hinsberg, W.; Houle, F.; Seidel, P.; Johnson, R.; Oldham, W. Thermal and Acid-Catalyzed Deprotection Kinetics in Candidate Deep Ultraviolet Resist Materials. *J. Vac. Sci. Technol., B* **1994**, *12*, 3857–3862.
- Thompson, L. F.; Willson, C. G.; Bowden, M. J. *Introduction to Microlithography*; American Chemical Society: Washington, DC, 1994; pp 212–232.

16. Flynn, J. H.; Wall, L. A. A Quick, Direct Method for the Determination of Activation Energy from Thermogravimetric Data. *J. Polym. Sci. Polym. Lett.* **1966**, *4*, 323–328.
17. Chenoweth, K. C.; Cheung, S.; van Dulin, A. C. T.; Goddard, W. A.; Kober, E. M. Simulations on the Thermal Decomposition of a Poly(dimethylsiloxane) Polymer Using the ReaxFF Force Field. *J. Am. Chem. Soc.* **2005**, *127*, 7192–7202.
18. Bershtein, V. A.; Ryzhov, V. A. Far Infrared Spectroscopy of Polymers. *Adv. Polym. Sci.* **1994**, *114*, 43–121.
19. Malik, S.; Eisele, J.; Whewell, A.; Ferreira, L.; Holt, T.; Bowden, M. Post-exposure Bake Temperature Considerations for High Activation Energy Resist Systems. *J. Photopolym. Sci. Technol.* **2000**, *13*, 513–518.
20. Kang, S.; Wu, W.; Choi, K.; Silva, A. D.; Ober, C. K.; Prabhu, V. M. Characterization of the Photoacid Diffusion Length and Reaction Kinetics in EUV Photoresists with IR Spectroscopy. *Macromolecules* **2010**, *43*, 4275–4286.
21. Kang, S. H.; Prabhu, V. M.; Vogt, B. D.; Lin, E. K.; Wu, W. L.; Turnquest, K. Effect of Copolymer Composition on Acid-Catalyzed Deprotection Reaction Kinetics in Model Photoresists. *Polymer* **2006**, *47*, 6293–6302.
22. Perera, G. M.; Pandey, Y. N.; Patil, A. A.; Stein, G. E.; Doxastakis, M. Reaction Kinetics in Acid-Catalyzed Deprotection of Polymer Films. *J. Phys. Chem. C* **2012**, *116*, 24706–24716.
23. Houle, F. A.; Hinsberg, W. D.; Morrison, M.; Sanchez, M. I.; Wallraff, G.; Larson, C.; Hoffagle, J. Determination of Coupled Acid Catalysis-Diffusion Processes in a Positive-Tone Chemically Amplified Photoresist. *J. Vac. Sci. Technol., B* **2000**, *18*, 1874–1885.
24. Kozawa, T.; Tagawa, S.; Santillan, J. J.; Toriumi, M.; Itani, T. Effects of Rate Constant for Deprotection on Latent Image Formation in Chemically Amplified Extreme Ultraviolet Resists. *Jpn. J. Appl. Phys.* **2008**, *47*, 4926–4931.
25. Kunz, R. R.; Downs, D. K. Outgassing of Organic Vapors from 193 nm Photoresists: Impact on Atmospheric Purity near the Lens Optics. *J. Vac. Sci. Technol., B* **1999**, *17*, 3330–3334.
26. Vogt, B. D.; Kang, S.; Prabhu, V. M.; Ashwin, R.; Lin, E. K.; Satija, S. K.; Turnquest, K.; Wu, W. The Deprotection Reaction Front Profile in Model 193nm Methacrylate-Based Chemically Amplified Photoresists. *Proc. SPIE* **2006**, *6153*, 615316.
27. Allinger, N. L.; Sprague, J. T. Conformational Analysis. LXXXIV. Study of the Structures and Energies of Some Alkenes and Cycloalkenes by the Force Field Method. *J. Am. Chem. Soc.* **1972**, *94*, 5734–5747.
28. Fredrickson, G. H.; Andersen, H. C. Kinetic Ising Model of the Glass Transition. *Phys. Rev. Lett.* **1984**, *53*, 1244–1247.
29. Ferry, J. D. *Viscoelastic Properties of Polymers*; John Wiley & Sons: New York, 1980; pp 264–315.
30. Priestly, R. D.; Broadbelt, L. J.; Torkelson, J. M.; Fukao, K. Glass Transition and α -Relaxation Dynamics of Thin Films of Labeled Polystyrene. *Phys. Rev. E* **2007**, *75*, 061806.
31. Bueche, F. *Physical Properties of Polymers*; Interscience: New York, 1962; pp 90–93.
32. Dektar, J. L.; Hacker, N. P. Photochemistry of Triarylsulfonium Salts. *J. Am. Chem. Soc.* **1990**, *112*, 6004–6015.